Sādhanā (2025) 50:193
https://doi.org/10.1007/s12046-025-02785-z

The effective temperature model applied to absorption cross section considering the Kaniadakis distribution

MARCELO V. SILVA[1,*], DIEGO GONCALVES[1], MARIA V. A. OLIVEIRA[1], FRANCK ROGER A. SILVA[1], MARCUS V. C. GÁLIA[2], GIOVANNI L. DE STEFANI[1] and DANIEL A. P. PALMA[3]

[1]Nuclear Engineering Program, COPPE/Universidade Federal do Rio de Janeiro, Rio de Janeiro 21.941-914, RJ, Brazil
[2]Instituto de Pesquisas Energéticas e Nucleares, IPEN/CNEN, Ãao Paulo, SP, Brazil
[3]Nuclear Institute of Engineering, CNEN, Rio de Janeiro 21.941-906, RJ, Brazil
e-mail: mvilela@coppe.ufrj.br; giovanni.laranjo@coppe.ufrj.br; daniel.palma@cnen.gov.br

MS received 14 November 2022; revised 2 May 2024; accepted 6 January 2025

Abstract. This paper presents an application of an approximate relationship be tween the Doppler broadening function based on the Maxwell-Boltzmann distribution and the deformed Doppler broadening function based on the generalized Kaniadakis distribution. The relationship is based on the effective temperature of the medium. The application is to the exemplary cases of the U-238, Th-232, and Pu-240nuclides. The straightforward implementation of the relationship demonstrates its suitability as a tool for diverse cross-section values. These values decrease with the expected attenuation of the peaks as the Kaniadakis κ value increases.

Keywords. Capture cross-section; effective medium temperature; deformed Doppler broadening function; maxwell-Boltzmann distribution; kaniadakis distribution.

1. Introduction

It is easy to think about the importance that energy resources occupy in the economy, in its most varied aspects, especially with regard to their decisive and strategic role for the economic development of a nation. The diffusion of energy forms was preponderant for the accelerated development of the modern world. The Figure 1 shows the countries of the world ranked according to per capita energy consumption (CPE). The color tone of the country corresponds to the magnitude of the indicator. The darker the color, the higher the value.

There is also a consensus that there is a direct relationship between energy consumption in a country and the Gross Domestic Product (GDP). Such statement is easily understood when we remember that a high GDP means a market strong enough to guarantee an equally heated consumption and an industrial sector capable of guaranteeing the transformation of primary goods into consumer goods, in a virtuous circle that leads to more economic growth and consequent positive variation of this GDP [2].

Once the relationship between a nation's economic growth and per capita energy consumption has been established, it is possible to see that the trend is for growth in energy demand and consequently in the ecological footprint left on the planet. The temporal evolution of world energy consumption per capita between 1979-2019 can be seen in figure 2.

Currently, the world energy matrix is increasingly diversified with the insertion and/or popularization of new technologies. However, a well-established technology can contribute to the reduction of greenhouse gas emissions and consequently to the reduction of the ecological footprint: nuclear energy. The figure 3 below shows the temporal evolution of the share of nuclear energy between the years 1975 and 2015.

Although it seems that power generation via nuclear fission is losing importance as time goes on, Nuclear energy plays an important role in the development of electric energy generation in the world, as the great world powers use this energy, not only to Produce electricity, but also to move ships, submarines, application in the medical area, in industry, etc. Updated data show that there are 439 reactor units in operation worldwide providing around 30% of the world's low carbon electricity which shows that nuclear energy can be part of the solution [5].

Of the 56 reactors currently under construction, 48 are of the PWR type, a well-established technology that has received several improvements, mainly after the lessons learned after Fukushima. Different designs of generation

*For correspondence
Published online: 20 August 2025

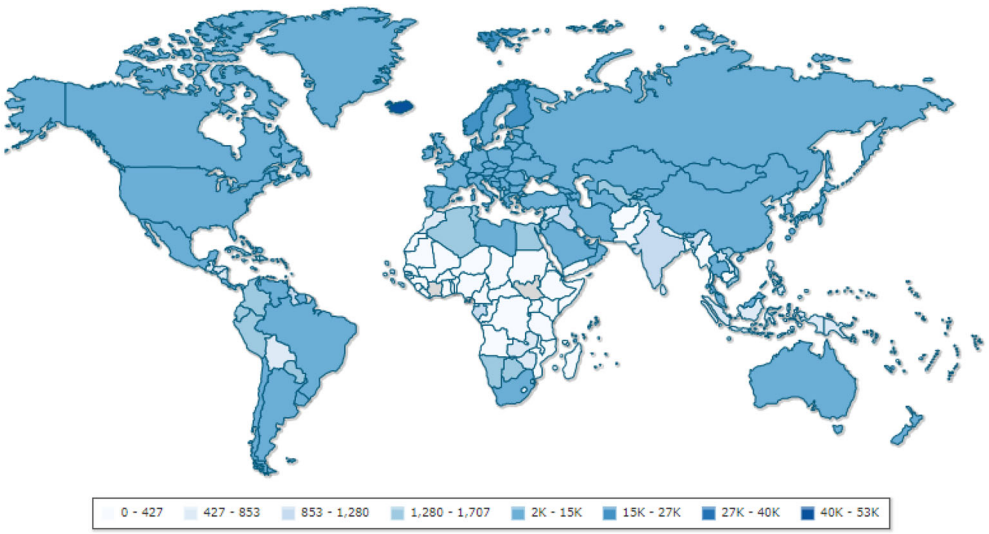

Figure 1. Electricity consumption per capita - World (January, 2020)[1].

III+ and IV reactors are under development, not to mention small modular reactors (SMR) [6–8], which leads to the development of calculation methodologies that consider different operating ranges regarding temperatures and transients.

In nuclear reactors, some neutrons can be absorbed in the resonance region, and accurate treatment of resonant absorptions is important as they vary with fuel temperature due to Doppler broadening. The thermal nuclei motion in the reactor core is properly represented in the microscopic cross section of the neutron-nucleus interaction through the Doppler Broadening Function $\psi(x,\xi)$, as well as in the Interference Term Function $\chi(x,\xi)$.

$$\overline{\sigma}_{\gamma}(E,T) = \sigma_0 \left(\frac{\Gamma_{\gamma}}{\Gamma}\right)\left(\frac{E_0}{E}\right)^{\frac{1}{2}} \psi(x,\xi). \tag{1}$$

The Doppler broadening function that uses the Maxwell-Boltzmann distribution of velocities is represented by Duderstadt and Hamilton [9],

$$\psi(x,\xi) = \frac{\xi}{2\sqrt{\pi}} \int_{-\infty}^{+\infty} \frac{dy}{1+y^2} \exp\left[\frac{-\xi^2}{4}(x-y)^2\right] \tag{2}$$

such that x, y and ξ are defined by:

- $x \equiv \frac{2}{\Gamma}(E - E_0)$;
- $\xi \equiv \frac{\Gamma}{\Gamma_D} = \frac{\Gamma}{(4E_0 k_B T/A)^{\frac{1}{2}}}$;
- $y \equiv \frac{2}{\Gamma}(E_{CM} - E_0)$;

where E is the incident neutron energy, E_{CM} is the center-of-mass energy, E_0 is the energy where the resonance occurs, Γ is total resonance width, Γ_D is the Doppler width of the resonance, T is the medium temperature and A the target nucleus mass number. The Doppler broadening function is only used in the $(\psi - \chi)$ method [9, 10]. Basically, this method uses the single-level resonance representation of cross sections based on the resonance parameters. Using the psi-chi method, the cross sections at 0 K are assumed to be composed of a series of single level Breit-Wigner resonances. Equation (2) is used in existing codes to calculate multigroup cross-sections, as for example [11–13].

The proposed method requires only 1.76 % of the computing time spent by the conventional Gauss-Legendre quadrature method (Silva, 2021). Reducing computational time in reactor calculations is very important in several methodologies that require hundreds of reactor calculations in series, as is the case for optimizing fuel reload with artificial intelligence [18, 28, 29, 31–33]. The results thus obtained are presented in their functional forms, as integrals without analytical solution. These have complicated structure, making the use of some approximations useful. Therefore, the concept of effective temperature aims to map the values obtained for the conventional Doppler broadening function, calculated at a temperature T, to an effective temperature T_{eff} in the system in which the velocity distribution is quasi-Maxwellian as in the Kaniadakis distribution [14–16].

The structure of this paper is as follows: Section 2 presents the conventional and Kaniadakis Doppler broadening functions. In section 3 the methodology of effective temperature of the medium is described. The results obtained in

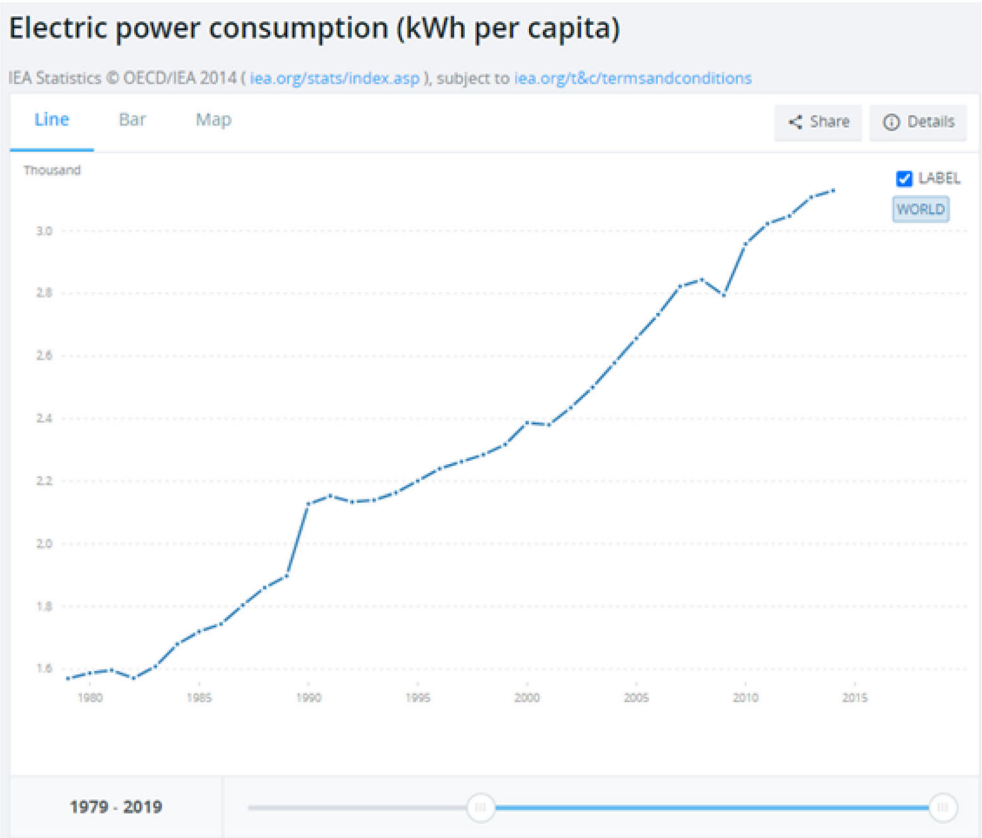

Figure 2. Electric power consumption (kWh per capita) [3].

the calculation of the resonant absorption cross sections using the proposed methodology for isotopes of interest are reported in section 4. Finally, in section 5 conclusions and suggestions for future work are presented.

2. Methodology

2.1 *The conventional and Kanidakis Doppler broadening functions*

Nuclear fuels consist of heavy nucleus that have complex nuclear structures whose microscopic cross sections have numerous resonances. Due to the Doppler Broadening phenomenon, the temperature variation causes, and precisely on the energy range of the nuclear resonances, a significant alteration on the neutron spectrum and, as a result, on the value for the multigroup cross-sections. The Maxwell-Boltzmann model considers the nuclei of a nuclear reactor as being one single gas whose molecules are thermally agitated at different speeds [19]. This molecule thermal agitation is described by the Maxwell-Boltzmann distribution:

$$f(V,T) = \left(\frac{M}{2\pi k_B T}\right)^{\frac{3}{2}} \exp\left(-\frac{MV^2}{2k_B T}\right). \tag{3}$$

In Equation (3), k_B represents the Boltzmann constant, M is the target nucleus mass, T is the temperature of the medium, and V is the velocity of the target nucleus. The Maxwell-Boltzmann distribution accurately describes the physical neutron-nucleus interaction phenomena in a condition of thermal equilibrium. However, the physical phenomena that lie outside the condition of thermal equilibrium cannot be described through Maxwell-Boltzmann statistics, making it necessary to use a generalised statistic. This generalisation has been the object of research work and continuous development, as seen, for example, in the papers of Tsallis [20, 30] and Kaniadakis [15, 16, 21].

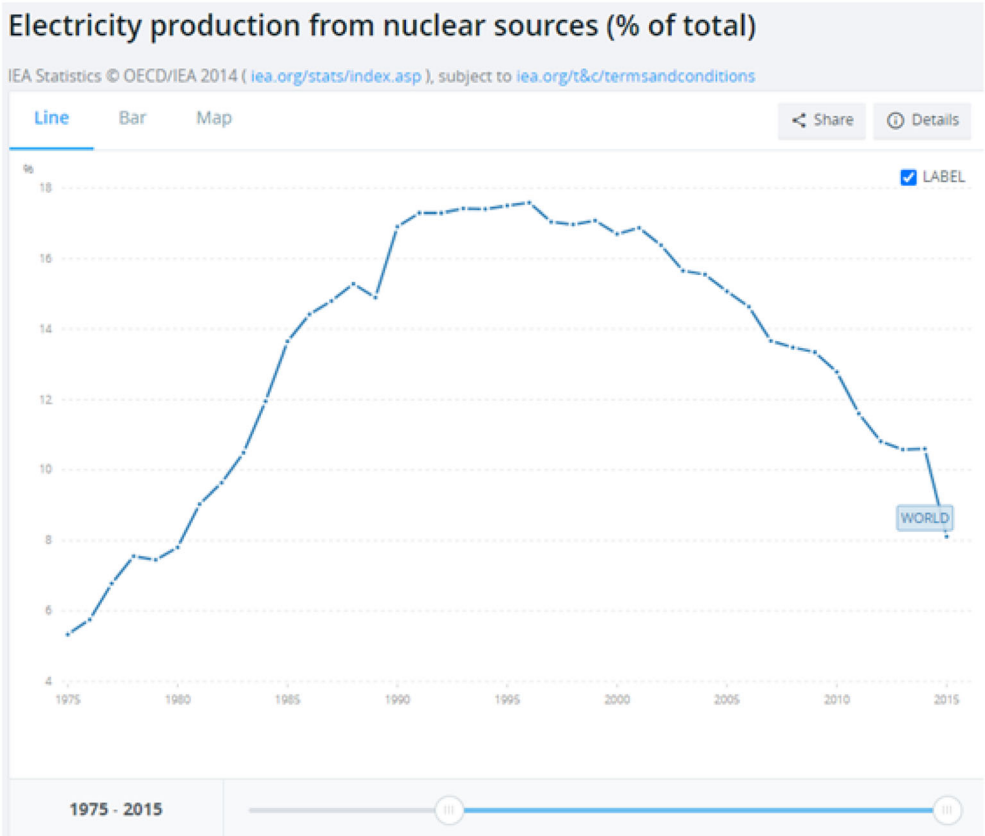

Figure 3. Electricity production from nuclear sources (% of total) [4].

The numerical solution of equation (2) demands considerable computing time and because of that several methods were developed to obtain analytical approximations for the Doppler broadening function, considering the standard Maxwell-Boltzmann statistics. Amongst the analytical approximations for the Doppler broadening function, we find the approximations proposed by Campos and Martinez [22]; Palma *et al* [23]; Gonçalves *et al* [24]; and Keshavamurthy and Harish [25]. In the first three articles the authors differentiating the integral expression of the Doppler broadening function in relation to x and found the following differential equation:

$$\frac{4}{\xi^2}\frac{\partial^2\psi(x,\xi)}{\partial x^2}+4x\frac{\partial\psi(x,\xi)}{\partial x}+\psi(x,\xi)(2+\xi^2x^2+\xi^2)=\xi^2, \tag{4}$$

subjected to the following initial conditions:

$$\left.\frac{\partial\psi(x,\xi)}{\partial x}\right|_{x=0}=\psi_0=\frac{\xi\sqrt{\pi}}{2}e^{\frac{\xi^2}{4}}\left[1-\operatorname{erf}\left(\frac{\xi}{2}\right)\right], \tag{5}$$

$$\left.\frac{\partial\psi(x,\xi)}{\partial x}\right|_{x=0}=0. \tag{6}$$

When solving equation (2) with the power series expansion method and Fourier series method the authors obtained analytical expressions for the Doppler broadening function.

In the paper by Keshavamurthy and Harish the 4-pole Padé method was used to obtain an analytical approximation for the Doppler broadening function $\psi(x,\xi)$ [25]. The 4-pole Padé approximation for $\psi(x,\xi)$ has the following expression:

$$\psi(x,\xi)\cong\frac{\xi\sqrt{\pi}}{2}\mathbb{R}\mathrm{e}[w(z)], \tag{7}$$

where

$$z=u+ih, \tag{8}$$

and,

$$\begin{cases} u = \dfrac{\xi x}{2}, \\ h = \dfrac{\xi}{2}. \end{cases} \tag{9}$$

Function $w(z)$ can be expressed using the terms of the 4-pole Padé polynomials Keshavamurthy and Harish [25] with the result that:

$$w(z) = \frac{i}{\sqrt{\pi}} \frac{p_0 + p_1 z + p_2 z^2 + p_3 z^3}{1 + q_1 z + q_2 z^2 + q_3 z^3 + q_4 z^4}. \tag{10}$$

In replacing equation (10) in equation (7) one gets the following expression for the Doppler broadening function $\psi(x, \xi)$:

$$\psi(x, \xi) \cong \frac{\xi\sqrt{\pi}}{2} \mathbb{R}e\left[\frac{i}{\sqrt{\pi}} \frac{p_0 + p_1 z + p_2 z^2 + p_3 z^3}{1 + q_1 z + q_2 z^2 + q_3 z^3 + q_4 z^4}\right]. \tag{11}$$

The coefficients for p_j and q_j are show on Table 1.

A first use of the Kaniadakis distribution in the context of nuclear engineering was done by Guedes *et al* [26]. Their paper presented a Deformed Doppler broadening function using the Kaniadakis distribution that describes neutron-nucleus interactions with and without the thermal equilibrium.

The results obtained by Guedes *et al*[26] and de Abreu *et al* [27] contributed to the ongoing investigation involving the Deformed Doppler broadening function in the domain of nuclear engineering with the use of Kaniadakis statistics.

Guedes *et al* [26] and de Abreu *et al* [27] provided numerical and analytical approximations, respectively, for the Deformed Doppler broadening function using the quasi-Maxwellian statistics of Kaniadakis, as represented by $\psi_\kappa(x, \xi)$. The Kaniadakis distribution is represented as follows:

$$f_\kappa(V, T) = A(\kappa) \exp_\kappa\left(\frac{-MV^2}{2k_B T}\right) \tag{12}$$

where,

$$A_\kappa = \left(\frac{|\kappa| M}{\pi K_B T}\right)^{\frac{3}{2}} \left(1 + \frac{3|\kappa|}{2}\right) \frac{\Gamma\left(\frac{1}{2|\kappa|} + \frac{3}{4}\right)}{\Gamma\left(\frac{1}{2|\kappa|} - \frac{3}{4}\right)}. \tag{13}$$

Moreover, the $\exp_\kappa$ (κ-exponential) function is defined by Kaniadakis et al. [16]:

$$\exp_\kappa(x) \equiv \left(\sqrt{1 + \kappa^2 x^2} + kx\right)^{\frac{1}{\kappa}}. \tag{14}$$

Using the Bethe-Placzek approximation Guedes et al. [26] obtained the Deformed Doppler Broadening Function, considering the Kaniadakis distribution:

Table 1. Coefficients p and q for the 4-pole Padé approximation [17]

$p_0 = -i\sqrt{\pi}$	$q_1 = \frac{-i(9\pi-28)\sqrt{\pi}}{2(6\pi^2-29\pi+32)}$
$p_1 = \frac{(15\pi^2-88\pi+128)}{(6\pi^2-29\pi+32)}$	$q_2 = \frac{(36\pi^2-195\pi+256)}{6(6\pi^2-29\pi+32)}$
$p_2 = \frac{-i(33\pi-104)\sqrt{\pi}}{6(6\pi^2-29\pi+32)}$	$q_3 = \frac{i(-33\pi+104)\sqrt{\pi}}{6(6\pi^2-29\pi+32)}$
$p_3 = \frac{(9\pi^2-69\pi+128)}{3(6\pi^2-29\pi+32)}$	$q_4 = \frac{(9\pi^2-69\pi+128)}{3(6\pi^2-29\pi+32)}$

$$\psi_\kappa(x, \xi) = \frac{\xi}{2\sqrt{\pi}} B(\kappa) \int_{-\infty}^{+\infty} \frac{dy}{1 + y^2} i exp_\kappa\left[\frac{-\xi^2 (x - y)^2}{4}\right] \tag{15}$$

where,

$$\begin{aligned} & i exp_\kappa\left(\frac{-\xi^2 (x-y)^2}{4}\right) \\ & \equiv \frac{\kappa^2\left(\frac{\xi^2(x-y)^2}{4}\right) + \sqrt{1 + \kappa^2\left(\frac{\xi^2(x-y)^2}{4}\right)^2}}{1 - \kappa^2} \times \\ & \times exp_\kappa\left(\frac{-\xi^2 (x-y)^2}{4}\right) \end{aligned} \tag{16}$$

and

$$B(\kappa) = (2|\kappa|)^{\frac{3}{2}} \left(1 + \frac{1}{2} 3|\kappa|\right) \frac{\Gamma\left(\frac{1}{2|\kappa|} + \frac{3}{4}\right)}{\Gamma\left(\frac{1}{2|\kappa|} - \frac{3}{4}\right)} \tag{17}$$

2.2 *The effective temperature model*

The model for effective medium temperature T_{eff} was proposed by da Silva et al. [17] that consists of determining the temperature T_{eff} that will have the Doppler broadening function with the Maxwell-Boltzmann distribution reproduced the same value for the function with the Kaniadakis distribution in the actual temperature T of the medium, that is:

$$\psi_\kappa(x, \xi) \cong \psi(x, \tilde{\xi}) \tag{18}$$

where:

$$\tilde{\xi} \equiv \frac{\Gamma}{\left(\frac{4E_0 k_B T_{eff}}{A}\right)^{1/2}}, \tag{19}$$

and

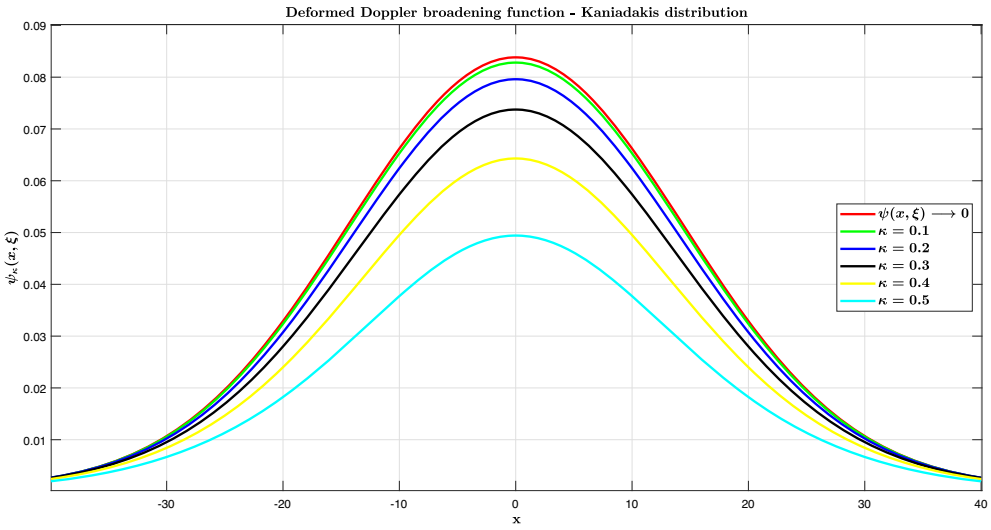

Figure 4. $\psi_\kappa(x, \xi=0.1)$ for different κ.

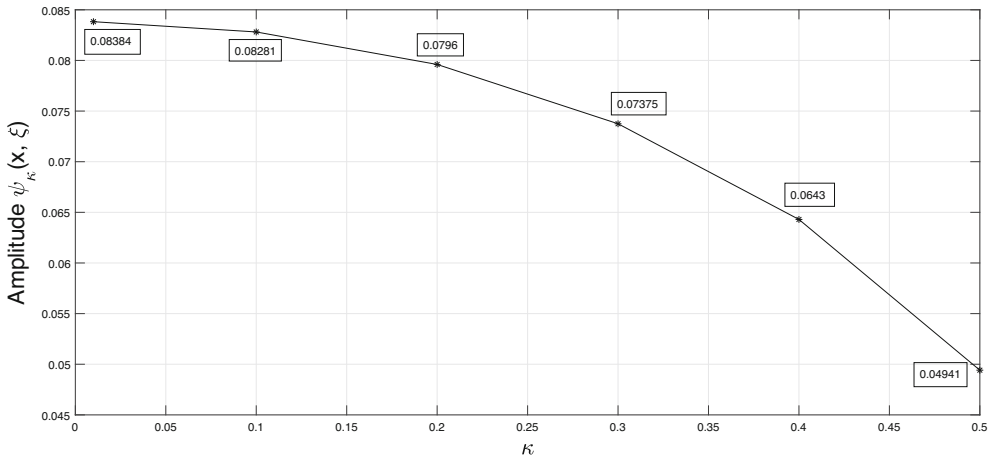

Figure 5. Peak values for $\psi_\kappa(x, \xi=0.1)$ as κ varies.

$$\xi \equiv \frac{\Gamma}{\left(\frac{4E_0 k_B T}{A}\right)^{1/2}}. \tag{20}$$

In using the approximation provided by equation (11) da Silva *et al* [17] one was obtain the value of $\tilde{\xi}$ which satisfies the following equation:

$$\psi_\kappa(x,\xi) \cong \frac{\tilde{\xi}\sqrt{\pi}}{2}\mathbb{R}e\left[\frac{i}{\sqrt{\pi}}\frac{p_0 + p_1\tilde{z} + p_2\tilde{z}^2 + p_3\tilde{z}^3}{1 + q_1\tilde{z} + q_2\tilde{z}^2 + q_3\tilde{z}^3 + q_4\tilde{z}^4}\right] \tag{21}$$

where

$$\tilde{z} = \tilde{u} + i\tilde{h}, \tag{22}$$

and

$$\begin{cases} \tilde{u} = \dfrac{\tilde{\xi}x}{2} \\ \tilde{h} = \dfrac{\tilde{\xi}}{2} \end{cases} \tag{23}$$

In general terms, tables were obtained for values of $\tilde{\xi}$ for different intervals of the variables κ, x and ξ, according to the analysis da Silva *et al* [17]:

Table 2. Nuclear parameters used in the calculation of $\overline{\sigma}_\gamma(E,T)$ for the first resonance of the isotopes

Isotopes	E_0 (eV)	Γ_n (eV)	$\Gamma_\gamma(eV)$	$\sigma_0(10^4\text{barns})$
^{238}U	6.67	0.00152	0.026	2.4
^{232}Th	23.43	0.039	0.0261	1.5
^{240}Pu	20.45	0.0027	0.0322	1.0

$$\tilde{\xi} = p_\kappa(x,\xi)\begin{cases} 0.1 \leqslant & \kappa & \leqslant 0.5 \\ 0 \leqslant & x & \leqslant 40 \\ 0.05 \leqslant & \xi & \leqslant 0.5 \end{cases} \tag{24}$$

Using a Genetic Algorithm as in the paper da Silva *et al* [17], the obtained data set was fitted to polynomial regression method of the form. he polynomials for κ = 0.1 and κ = 0.2 can be written as follows:

$$\begin{aligned}\tilde{\xi}_{\kappa=0.1}(x,\xi) = &-0.0095668 + 0.0042817x + 1.2301\xi \\ &+ 0.00025628x^2 - 0.1449x\xi - \\ &- 1.2704\xi^2 - 6.1751\times10^{-5}x^3 \\ &+ 0.0062072x^2\xi \\ &+ 0.92537x\xi^2 + 0.76292\xi^3 + \\ &+ 2.9873\times10^{-6}x^4 - 0.00010748x^3\xi \\ &- 0.023709x^2\xi^2 - 2.1902x\xi^3 + 6.4376\xi^4 - \\ &- 4.1619\times10^{-8}x^5 + 8.0913\times10^{-7}x^4\xi \\ &+ 0.00015675x^3\xi^2 + 0.023925x^2\xi^3 + \\ &+ 1.7734x\xi^4 - 9.4704\xi^5,\end{aligned} \tag{25}$$

$$\begin{aligned}\tilde{\xi}_{\kappa=0.2}(x,\xi) = &0.0046822 + 0.0030388x^1 \\ &+ 0.73111\xi - 0.00042548x^2 \\ &- 0.057383x\xi + 2.8556\xi^2 + 1.4651\times10^{-5}x^3 \\ &+ 0.0066264x^2\xi + 0.25925x\xi^2 - \\ &- 14.631\xi^3 + 1.8425\times10^{-8}x^4 \\ &- 0.00025003x^3\xi - 0.011772x^2\xi^2 - \\ &- 0.61369x\xi^3 + 31.818\xi^4 - 4.1333\times10^{-9}x^5 \\ &+ 2.9973\times10^{-6}x^4\xi + \\ &+ 0.00013975x^3\xi^2 + 0.0080984x^2\xi^3 \\ &+ 0.50658x\xi^4 - 24.629\xi^5.\end{aligned} \tag{26}$$

Thus, the deformed Doppler broadening function $\psi_\kappa(x,\xi)$, according to the Kaniadakis distribution, can be directly obtained using the conventional Doppler function $\psi(x,\tilde{\xi}_\kappa)$.

3. Results and discussion

In a preliminary analysis of the deformed Doppler broadening function's behaviour, using the Kaniadakis statistics, an overall curve attenuation was noticed for increasing values of the κ parameter. In other words, the resonance amplitude decreases. This fact is illustrated by the plots of Figure 4, where the distribution tend towards the conventional function as $\kappa \to 0$.

The peak values for $\psi_\kappa(x,\xi)$ were plotted in Figure 5 for selected κ, to further illustrate the attenuation of the resonance amplitude.

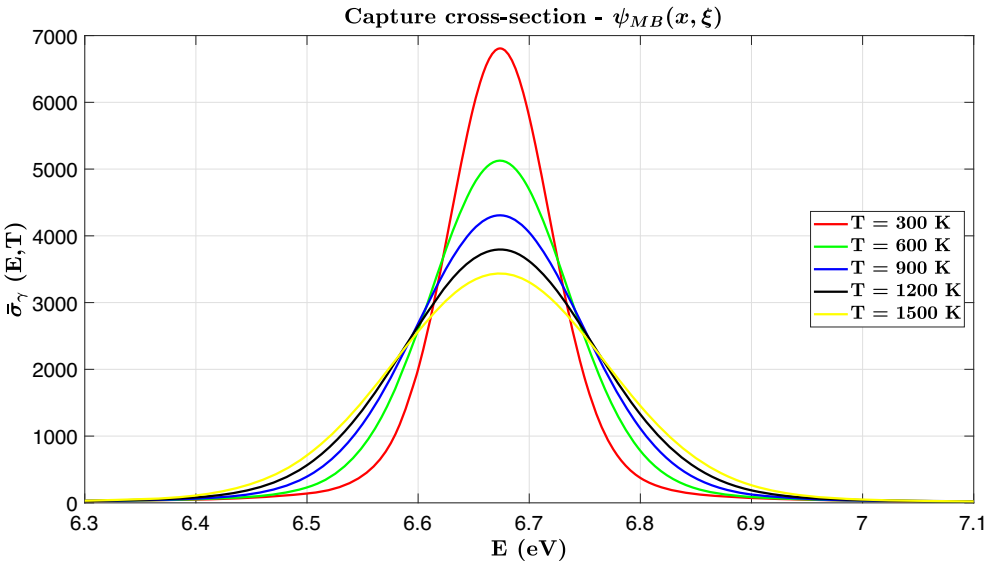

Figure 6. Capture cross-section resonance of the ^{238}U with $E_0 = 6.67$ (eV), as calculated by Eq. (2).

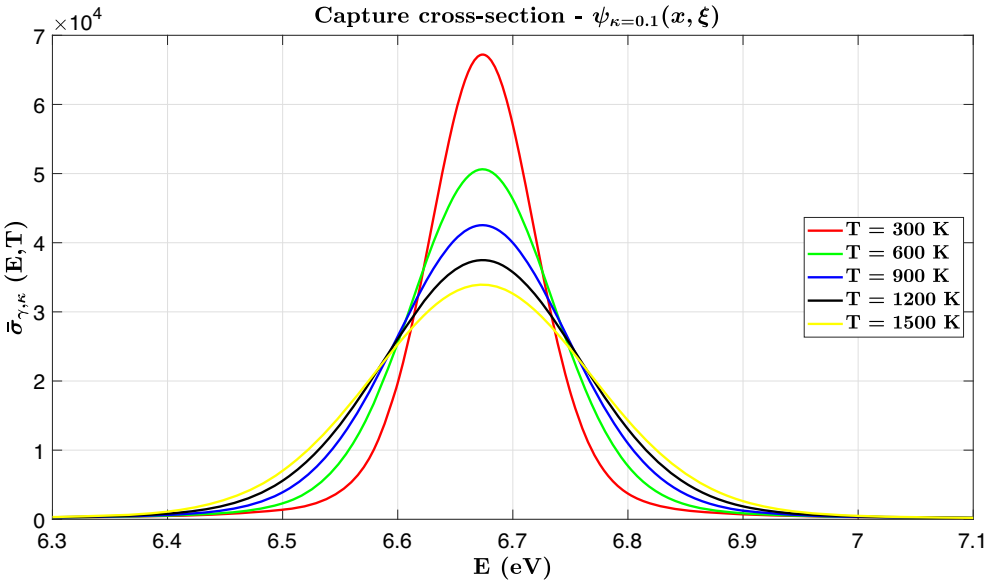

Figure 7. Capture cross-section resonance for the ^{238}U $E_0 = 6,67\ (eV)$, as calculated by Eq. (15).

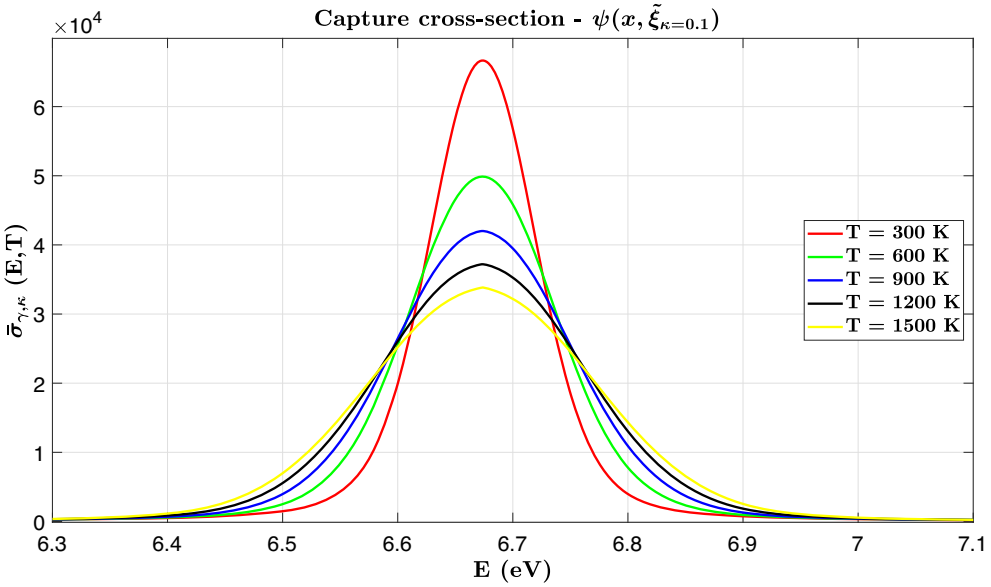

Figure 8. Capture cross-section resonance for the ^{238}U $E_0 = 6.67\ (eV)$, as calculated by Eq. (25).

As an application, the capture cross-section was calculated for the first resonance of the ^{238}U, ^{232}Th, and ^{240}Pu isotopes, using for different energies of incident neutrons from the known expression (1). (Furthermore, the deformed functions, according to the Kaniadakis distribution, see figures 9–12).

$$\underbrace{\psi(x,\xi) \equiv \psi_{MB}(x,\xi)}_{\text{Maxwell}-\text{Boltzmanndistribution}} \begin{cases} \psi_\kappa(x,\xi) & \text{Kaniadakis statistics distribution} \\ \psi(x,\tilde{\xi}) & \text{Effective temperature of the medium } T_{eff} \end{cases}$$

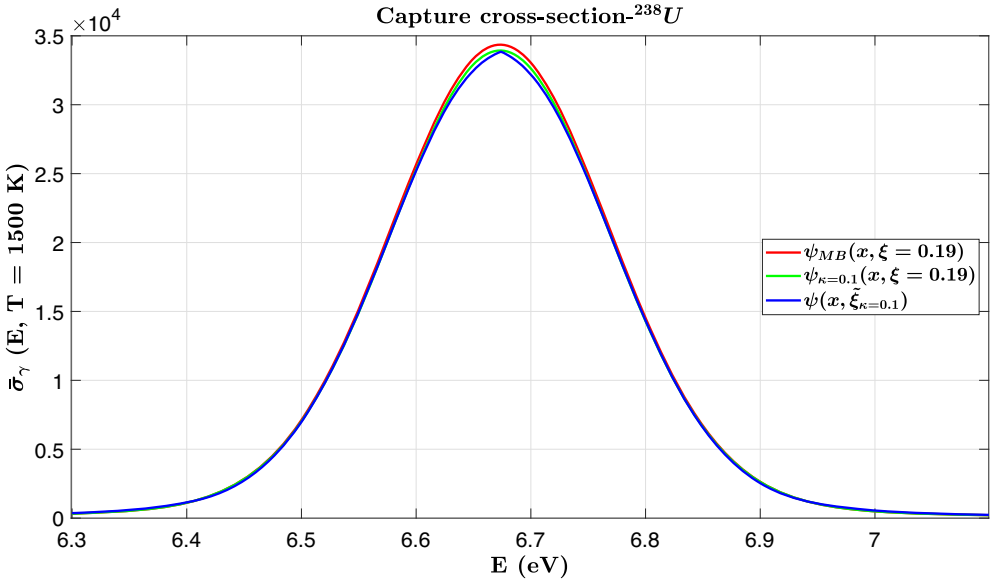

Figure 9. Capture cross-section resonance for the ^{238}U and $E_0 = 6.67\ (eV)$ considering $\kappa = 0.1$.

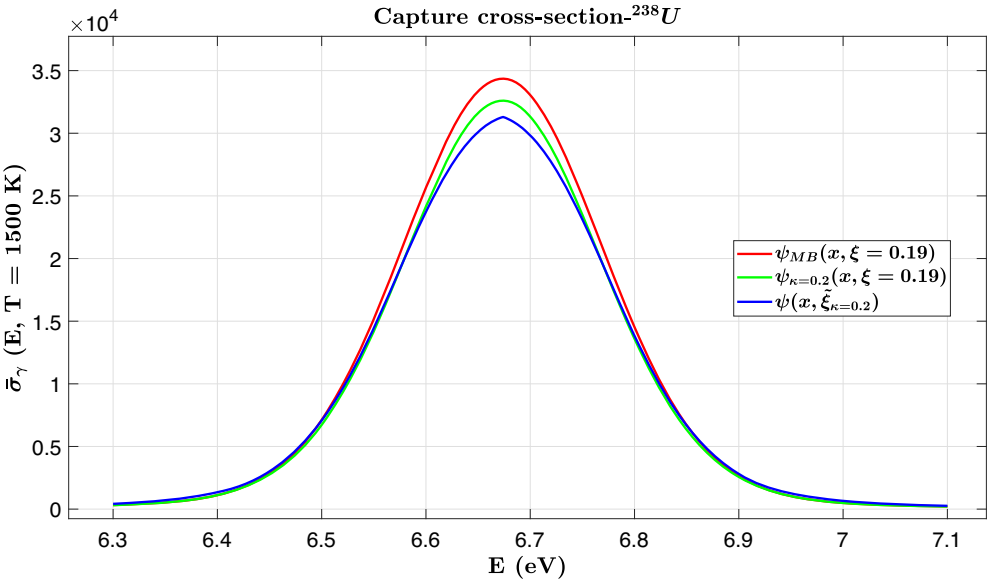

Figure 10. Capture cross-section resonance for the ^{238}U and $E_0 = 6.67\ (eV)$ considering $\kappa = 0.2$.

The deformed Doppler broadening function $\psi_\kappa(x, \xi)$ is approximated by the Doppler broadening function $\psi(x, \tilde{\xi})$, where ξ is associated to the temperature of medium T and $\tilde{\xi}$ relates to the effective temperature of medium T_{eff}. For calculation the capture cross-sections, it will only be necessary to replace T with T_{eff}. That is, the equation (19) may be rewritten as:

$$T_{ef} \equiv \frac{A\Gamma^2}{4k_B E_0 \tilde{\xi}^2} \tag{27}$$

In the next section, the results for the calculation of the mean capture cross-section are presented for different nuclides of importance in the physics of nuclear reactors. The parameters characterizing the first resonance line for these nuclides are presented in Table 2.

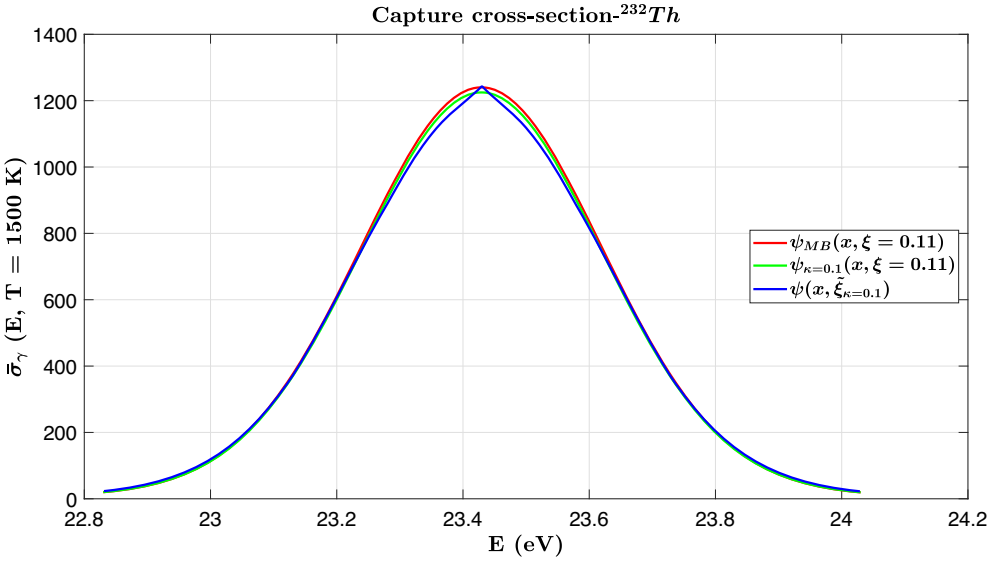

Figure 11. Capture cross-section resonance for the ^{232}Th and $E_0 = 23.43\ (eV)$ considering $\kappa = 0.1$.

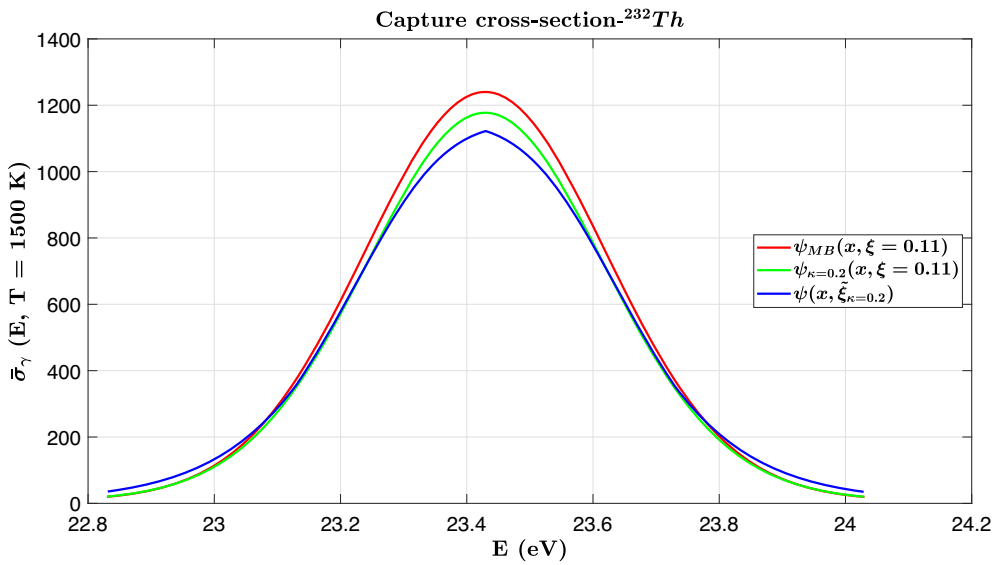

Figure 12. Capture cross-section resonance for the ^{232}Th and $E_0 = 23.43\ (eV)$ considering $\kappa = 0.2$.

3.1 *Capture cross-section* $\overline{\sigma}_\gamma(E, T)$

First, the mean capture cross-section was calculated using the conventional broadening function $\psi_{MB}(x, \xi)$ equation (2). For the ^{238}U nuclide, the results are shown in figure 6, for temperatures ranging from 300 K to 1500 K.

Analyzing the graph of the figure 6, we observe that the area under the cross section curve is conserved when temperature varies. furthermore, if the maximum of the resonance decreases, its width will tend to increase, as predicted by the Doppler effect. Hence, function contains positive values and the function is symmetric about the vertical axis.

3.2 *Deformed capture cross-section* $\overline{\sigma}_{\gamma,\kappa}(E, T)$

Similarly, in analysing the graphs shown in figure 7 and 8 maintaining the behavior described in 6, it is possible to see that for capture cross-sections were calculated using the deformed functions $\psi_\kappa(x, \xi)$ and $\psi(x, \tilde{\xi}_\kappa)$, respectively. (See figures 9–12).

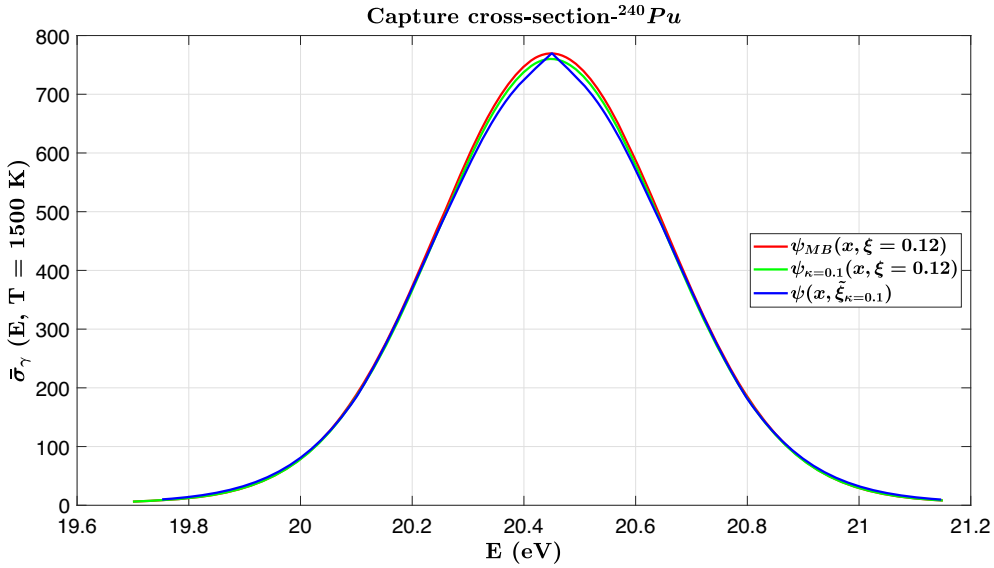

Figure 13. Capture cross-section resonance for the ^{240}Pu and $E_0 = 23.43\ (eV)$ considering $\kappa = 0.1$.

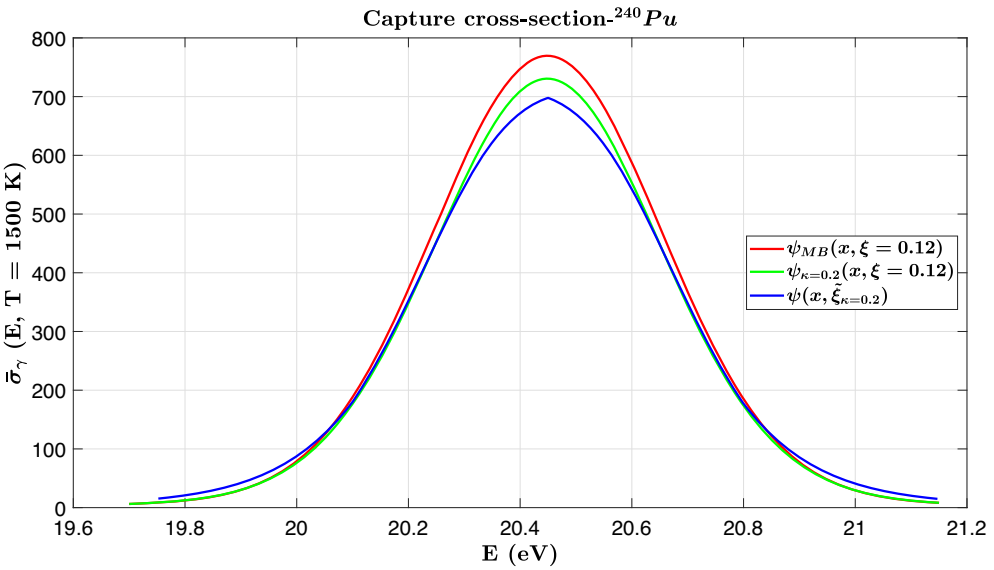

Figure 14. Capture cross-section resonance for the ^{240}Pu and $E_0 = 23.43\ (eV)$ considering $\kappa = 0.2$.

For the 1500 K temperature, typical in the fuel rods in PWR-type power reactor. The nuclear parameters used in these calculations are found in Table 2, and the graphs clearly show the influence of κ as it increases its deformation, as follows:

The results presented in figure 15 are relative to the peak values of the Deformed Doppler broadening function, using equation (15) and the proposed methodology, based on the effective temperature of the medium T_{eff}, combining equations (25) and (26). It is possible to see by the graph in the figure 15 that uranium cross sections is by far higher than plutonium and thorium.

It is possible to see by the graph of figure 15 that the ^{238}U cross-section (black curve) is almost two orders of

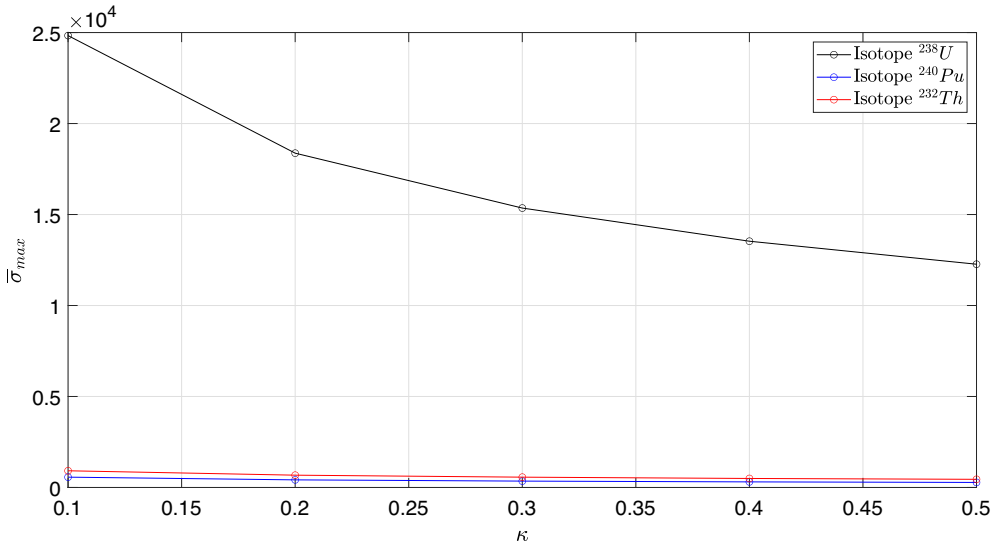

Figure 15. Capture cross-section resonance.

magnitude higher than the ^{240}Pu (blue) and the ^{232}Th (red) ones. This suggests that simulations, as a first step, may use equilibrium statistics for nuclides other than ^{238}U.

4. Conclusion

Considering that the medium is in thermal equilibrium, it is valid to use the Maxwell-Boltzmann statistic to represent the distribution of target nuclei velocities, used to obtain the Doppler broadening function, $\psi(x, \xi)$.

The Kaniadakis statistic can be used to obtain a deformed Doppler broadening function $\psi_\kappa(x, \xi)$, which has no analytical solution. For its calculation, the effective temperature model provides an approximate method, by finding a T_{eff} which maps this function to the conventional Doppler broadening function.

Due to its simplicity, the effective temperature model proves to be a suitable tool for out-of-equilibrium simulations. In addition, computational gain without significant loss of accuracy and avoiding reprogramming of existing subroutines.

Considering the isotopes ^{238}U, ^{232}Th, and ^{240}Pu, the results obtained show deviations of 1.5% for $\kappa = 0.1$ and up to 9% for $\kappa \leq 0.2$.

Acknowledgements

We would like to thank the CNPq and FAPERJ for Financial Support.

Declarations

Conflicts of interest The authors declare no conflict of interest.

References

[1] IndexMundi: Electricity consumption per capita – World. Available online: https://www.indexmundi.com. (accessed on 11 August 2022). Available online: https://www.indexmundi.com

[2] Šlaus I and Jacobs G 2011 Human capital and sustainability. *Sustainability* 3(1): 97–154. https://doi.org/10.3390/su3010097

[3] DataBank: Electric power consumption (kWh per capita). Available online: https://data.worldbank.org. (accessed on 11 August 2022). Available online: https://data.worldbank.org

[4] DataBank: Electricity production from nuclear sources (% of total). Available online: https://data.worldbank.org. (accessed on 11 August 2022). Available online: https://data.worldbank.org

[5] Wu J, Chen J, Zou C and Li X 2022 Accident modeling and analysis of nuclear reactors. *Energies* 15(16): 5790. https://doi.org/10.3390/en15165790

[6] Singh O M P and Singh R S 1989 Inherent safety concepts in nuclear power reactors. *Sadhana* 14(1): 1–20. https://doi.org/10.1007/bf02745340

[7] Cheng X 2007 Studies on advanced water-cooled reactors beyond generation III for power generation. *Frontiers of Energy and Power Engineering in China* 1(2): 141–149. https://doi.org/10.1007/s11708-007-0018-6

[8] Nayak A and Dutta B 2013 Nuclear power programme in india-past, present and future foreword. In: SADHANA-ACADEMY PROCEEDINGS IN ENGINEERING SCIENCES, vol. 38, pp. 773–774 . INDIAN ACAD SCIENCES CV RAMAN AVENUE, SADASHIVANAGAR, PB# 8005, BANGALORE ..

[9] Duderstadt J J and Hamilton L J 1976 Nuclear Reactor Analysis. Wiley, New York

[10] Yesilyurt G, Martin W R and Brown F B 2012 On-the-fly Doppler broadening for Monte Carlo codes. *Nuclear Science*

and Engineering 171(3): 239–257. https://doi.org/10.13182/nse11-67

[11] Hutchins B, Cowan C, Kelley M and Turner J 1971 ENDRUN-II: A COMPUTER CODE TO GENERATE A GENERALIZED MULTIGROUP DATA FILE FROM ENDF/B. General Electric Co., Sunnyvale, Calif. Breeder Reactor Dept. https://doi.org/10.2172/4739228

[12] Greene N, Lucius J, Petrie L, Ford III W, White J and Wright R 1976 AMPX: A Modular Code System for Generating Coupled Multigroup Neutron-gamma Libraries from ENDF/B. Oak Ridge National Lab., Tenn. (EUA)

[13] Tada K, Nagaya Y, Kunieda S, Suyama K and Fukahori T 2017 Development and verification of a new nuclear data processing system FRENDY. *Journal of Nuclear Science and Technology* 54(7): 806–817

[14] Kaniadakis G 2001 H-theorem and generalized entropies within the framework of nonlinear kinetics. *Physics Letters A* 288(5–6): 283–291. https://doi.org/10.1016/s0375-9601(01)00543-6

[15] Kaniadakis G 2002 Statistical mechanics in the context of special relativity. *Physical Review E* 66(5): 056125. https://doi.org/10.1103/PhysRevE.66.056125

[16] Kaniadakis G, Scarfone A, Sparavigna A and Wada T 2017 Composition law of κ-entropy for statistically independent systems. *Physical Review E* 95(5): 052112. https://doi.org/10.1103/PhysRev.E.95.052112

[17] Silva M V, Martinez A S and Gonçalves A C 2021 Effective medium temperature for calculating the doppler broadening function using Kaniadakis distribution. *Annals of Nuclear Energy* 161: 108500. https://doi.org/10.1016/j.anucene.2021.108500

[18] Moura Meneses A A and Schirru R 2015 A cross-entropy method applied to the in-core fuel management optimization of a pressurized water reactor. *Progress in Nuclear Energy* 83: 326–335. https://doi.org/10.1016/j.pnucene.2015.04.007

[19] Pathria R K 1996 Statistical Mechanics. Butterworth-Heinemann

[20] Tsallis C 1988 Possible generalization of Boltzmann-Gibbs statistics. *Journal of Statistical Physics* 52(1–2): 479–487. https://doi.org/10.1007/bf01016429

[21] Kaniadakis G 2005 Statistical mechanics in the context of special relativity. II. *Physical Review E* 72(3): 036108. https://doi.org/10.1103/PhysRevE.72.036108

[22] Campos T P R and Martinez A S 1987 The dependence of practical width on temperature. *Annals of Nuclear Energy* 14(5): 241–247. https://doi.org/10.1016/0306-4549(87)90045-4

[23] Palma D A P, Martinez A S and Silva F C 2006 The derivation of the doppler broadening function using Frobenius method. *Journal of Nuclear Science and Technology* 43(6): 617–622. https://doi.org/10.1080/18811248.2006.9711141

[24] Gonçalves Ad C, Martinez A S and Silva F C 2008 Solution of the Doppler broadening function based on the fourier cosine transform. *Annals of Nuclear Energy* 35(10): 1878–1881. https://doi.org/10.1016/j.anucene.2008.04.003

[25] Keshavamurthy R and Harish R 1993 Use of padé approximations in the analytical evaluation of the j (θ, β) function and its temperature derivative. *Nuclear Science and Engineering* 115(1): 81–88. https://doi.org/10.13182/NSE93-A35526

[26] Guedes G, Gonçalves A C and Palma D A 2017 The doppler broadening function using the kaniadakis distribution. *Annals of Nuclear Energy* 110: 453–458. https://doi.org/10.1016/j.anucene.2017.06.057

[27] Abreu W V, Gonçalves A C and Martinez A S 2019 Analytical solution for the doppler broadening function using the kaniadakis distribution. *Annals of Nuclear Energy* 126: 262–268. https://doi.org/10.1016/j.anucene.2018.11.023

[28] Silva M V, Schirru R, de Stefani G L, Nicolau A S, de Lima A M M, Pereira C M N A, Guimaraes J V S A, Gonçalves D M E (2024). Optimized modular nuclear reactor project utilizing artificial intelligence: Seed-blanket concept. Nuclear Engineering and Design, 423, 113187. https://doi.org/10.1016/j.nucengdes.2024.113187

[29] dos Santos, T. A., Genezini, F. A., & de Stefani, G. L. (2023). Optimization of IEA-R1 reactor core parameters using the particle swarm algorithm. Nuclear Engineering and Design, 415, 112713. https://doi.org/10.1016/j.nucengdes.2023.112713

[30] Silva, M. V., de Stefani, G. L., Guedes, G., & Palma, D. A. P. (2023). Effective medium temperature for calculating the deformed Doppler broadening function considering the Tsallis distribution. Annals of Nuclear Energy, 194, 110110. https://doi.org/10.1016/j.anucene.2023.110110

[31] Dasgupta, S. (1994). Understanding design: Artificial intelligence as an explanatory paradigm. Sadhana, 19(1), 5–21. https://doi.org/10.1007/BF02760388

[32] Manupati, V. K., Rajyalakshmi, G., Chan, F. T. S., & Thakkar, J. J. (2017). A hybrid multi-objective evolutionary algorithm approach for handling sequence- and machine-dependent set-up times in unrelated parallel machine scheduling problem. Sādhanā, 42(3), 391–403. https://doi.org/10.1007/s12046-017-0611-2

[33] de Oliveira, I. M. S., & Schirru, R. (2011). Swarm intelligence of artificial bees applied to in-core fuel management optimization. Annals of Nuclear Energy, 38(5), 1039–1045. https://doi.org/10.1016/j.anucene.2011.01.009